COMPUTATION OF EDDY CURRENTS IN HIGHLY CONDUCTIVE PARTICLES DISPERSED IN A MODERATELY CONDUCTIVE MATRIX

E. Rognin[1], G. Barba Rossa [1*], P. Brun[1], E. Sauvage[1], J. Lacombe[1]

[1]CEA, DEN, DTCD, SCDV, LDPV
BP 17171, F-30207 Bagnols-sur-Ceze, France
*guillaume.barbarossa@cea.fr; phone: +33 466 797 694; fax: +33 466 796 030

ABSTRACT. In this article, we report 3D numerical simulations of highly conductive non-magnetic particles dispersed in a moderately conductive matrix, subject to an AC magnetic field in a range of several hundred kHz. We address the issue of the scaling of current loops and heating power with respect to the volume fraction of the dispersed phase. Simulations are performed in two steps. First, a static electric potential gradient is imposed between two opposite faces of the simulation domain and an effective conductivity is computed in good agreement with percolation models. Second, the particles are constrained in a spherical sub-region and an AC magnetic field is imposed at the boundary of the domain. For small volume fractions, the induced Joule power is in good agreement with an analytical model of dilute dispersions. As the volume fraction increases, wider current loops form, until the percolation threshold is reached. Then the induced power in the spherical aggregate is well described by the power induced in an equivalent sphere with a volume-fraction-dependent conductivity.

INTRODUCTION

Electromagnetic induction heating of heterogeneous materials has been an active field of research for decades. In domains as diverse as polymer composites [1-3], civil engineering [4, 5], chemistry [6], electronics [7], or medicine [8], a conductive dispersed phase is used to convert electromagnetic energy into heat. Generally, the conductive phase is a dispersion of magnetic particles such as iron, or an entanglement of carbon fibres for higher frequency applications. However, few studies focus on non-magnetic conductive particles, although they can play a significant role in induction heating processes where temperature exceeds the Curie point, or where multiphase melts are involved [9-11].

Besides, from a theoretical point of view, the effective conductivity of composite materials has been thoroughly investigated through homogenization and percolation theories (see for example [12, 13]). Nevertheless, few authors reported studies on the theoretical scaling of the induced Joule power in the presence of an AC magnetic source [14-16].

In this article, we report 3D numerical simulations of eddy currents in highly conductive non-magnetic particles (typically metallic inclusions) dispersed in a moderately conductive matrix (typically a glass melt of conductivity 1 to 10 S/m), subject to an AC magnetic field in a range of several hundred kilohertz. Here, we address the issue of the scaling of current loops and heating power with respect to the volume fraction of the dispersed phase.

The paper is organized as follows: in the next section, we present a theoretical approach of the induction heating of dilute dispersions, followed by a description of the simulation

process. Then, we present the results of the simulations and compare the data to the models. Finally, we draw some concluding remarks.

MODEL AND SIMULATION

Induction heating of a dilute dispersion of spheres

We consider a non-magnetic conductive sphere, of conductivity σ and radius a, suspended in vacuum, and subject to an AC magnetic induction field of magnitude B and angular frequency ω. We assume that $a \ll c/\omega$, with c the speed of light, in other words we assume that the electromagnetic field is quasi-static. The time-averaged electromagnetic power, P, dissipated in the sphere is [17]:

$$P = \frac{2\pi\delta^3\omega B^2}{15\mu_0} f\left(\frac{a}{\delta}\right), \tag{1}$$

where μ_0 is the vacuum permeability, δ is the skin depth defined as $\delta = \sqrt{2/\sigma\mu_0\omega}$, and f is a dimensionless function of the normalized radius a/δ, such that:

$$f\left(\frac{a}{\delta}\right) = \frac{15}{2}\left(\frac{a}{\delta}\right)^3 \mathrm{Im}\left(\frac{j_2[(1+i)a/\delta]}{j_0[(1+i)a/\delta]}\right), \tag{2}$$

where j_n represents the spherical Bessel function of the first kind of order n. The function f, plotted in figure 1a, takes the value 1 for $a = \delta$, and is an increasing function of a/δ. Due to the skin effect, the scaling is different for $a \ll \delta$, where the heating power increases as $(a/\delta)^5$, and $a \gg \delta$, where the exponent is reduced to 2.

Now, we consider a dilute dispersion of such spheres, assuming that each sphere is not influenced by its neighbors. With φ the volume fraction occupied by the spheres, the time-averaged electromagnetic power, P_v, dissipated by unit of volume of the effective medium is:

$$P_v = \frac{\omega B^2}{10\mu_0}\varphi\, g\left(\frac{a}{\delta}\right), \tag{3}$$

with g a dimensionless function of a/δ defined by:

$$g\left(\frac{a}{\delta}\right) = \left(\frac{a}{\delta}\right)^{-3} f\left(\frac{a}{\delta}\right). \tag{4}$$

The function g is plotted on figure 1b. It has a maximum where a is of the order of δ. In other words, the dissipation of electromagnetic power in the dispersion reaches a maximum when the particle size is of the same order of magnitude as the skin depth in the particles.

The theory developed above may be valid only for dilute dispersions. On the other hand, as the volume fraction of the conductive phase grows, particles touch and form bigger and bigger clusters. Larger and larger current loops will develop, and the scaling of the heating power should be different from the dilute model, as we will see below. In this paper, we use numerical simulations to investigate this phenomenon. The next subsections will describe the simulation process.

Materials description

The electromagnetic field is solved at the scale of the particles. The particles are randomly distributed without exclusion constraint. Overlapping particles of constant diameter give a fair approximation of a random material [13]. An example of dispersion is reported in figure 2.

The normalized conductivity is $\sigma_0 = 1$ in the matrix and $\sigma_1 = 10^6$ in the dispersed phase. This ratio is typically encountered when dealing with a metallic phase, of conductivity around 10^6 S/m at high temperature, dispersed in a glass melt of conductivity 1 to 10 S/m.

The conductivity field is mapped on a 3D rectangular mesh of 100^3 cells. The particle radius is set to two hundredths (0.02) of the whole simulation box. The mesh is refined near the particles interface, up to 3 levels of recursion, in order to get a good resolution of the particles. By such means, a single particle contains around 16700 cells instead of 34 without refinement (see figure 2b).

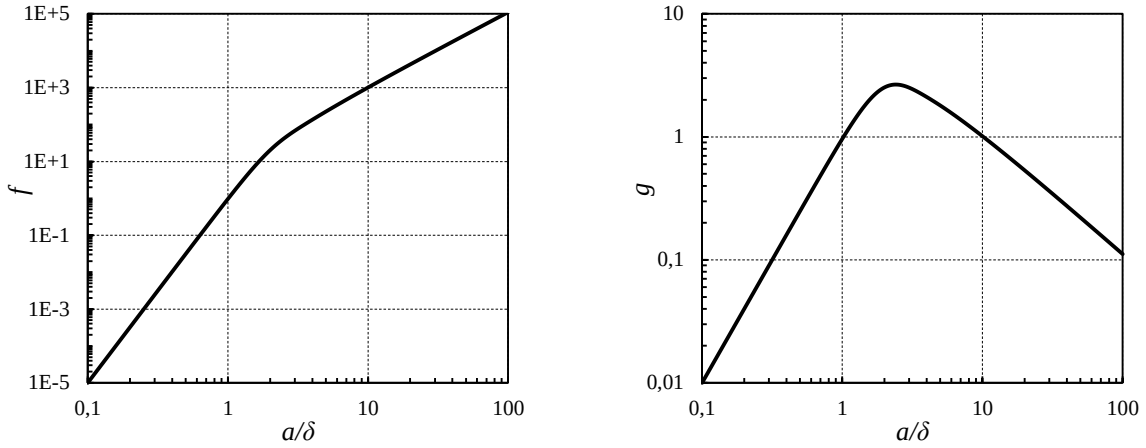

a. Function *f*. b. Function *g*.

Figure 1. Plot of the scaling functions *f* and *g*.

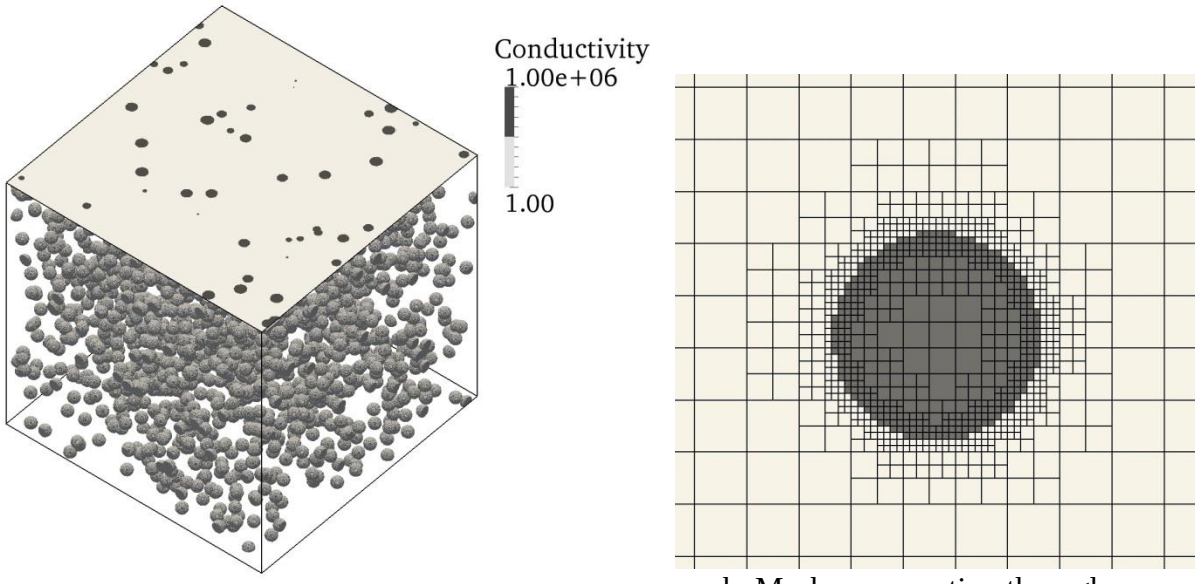

a. Simulation domain. b. Mesh cross section through a particle.

Figure 2. Simulated dispersion of volume fraction 6%.

Simulation strategy

The electromagnetic scalar and vector potentials are solved in the frequency domain by a collocated finite volume method inspired by [18, 19] who solved static electric fields for electrohydrodynamics applications. Here, we extend their approach to quasi-static sinusoidal fields. According to the theory of induction, the complex magnetic vector potential **A** must satisfy:

$$\nabla^2\mathbf{A} - \nabla\nabla\cdot\mathbf{A} = -\mu_0\mathbf{J}\,, \tag{5}$$

where **J** is the cell-centred electric current given by Ohm's law for conductors at rest:

$$\mathbf{J} = \sigma\mathbf{E} = \sigma(-\nabla V - i\omega\mathbf{A})\,, \tag{6}$$

where **E** is the electric field and *V* is the electric scalar potential. The zero divergence of **J** is insured if the scalar potential satisfies:

$$\nabla\cdot\left(\sigma_f\nabla V\right) = -i\omega\nabla\cdot(\sigma\mathbf{A})\,, \tag{7}$$

with σ_f the harmonic-interpolated value of the conductivity at cell faces. The solver has been implemented within the framework of the OpenFOAM® 2.3 finite volume library [20]. The coupled equations 5 and 7 are sequentially solved until global convergence is reached.

Generally, a gauge condition for the vector potential (typically the Coulomb gauge for induction heating) has to be enforced in order to ensure the uniqueness of the potentials. Nevertheless, we found that this procedure was not necessary in our simulation. The divergence of the vector potential is instead treated as an explicit source term without significantly hindering the convergence speed of the solution. In addition, the high conductivity ratio between the matrix and the particle yields ill-conditioned discretization matrices of equation 7. We employed a diagonal incomplete Cholesky preconditioner in pair with a multigrid solver, and set the tolerance on residuals to 10^{-6}.

Simulations are performed in two steps. First, particles are distributed across the whole simulation domain and a static electric potential gradient is imposed between two opposite faces of the mesh. An effective conductivity is computed from the total electric current flowing through the material. Second, the particles are constrained in a spherical sub-region and an AC magnetic field is imposed at the boundary of the domain. The time-averaged Joule loss is integrated over space and divided by the volume of the sub-region.

Due to the volume representation of the conductive particles, the frequency has to be set low enough that the skin depth exceeds several cell lengths. Since particles themselves are smaller than a dozen cells, the skin depth has the be larger than the particle size, in other words $\delta \geq a$. For a metallic particle of conductivity 10^6 S/m, at 100 kHz, the skin depth is 1.6 mm. Thus, for sub-millimetre particles, the volume description of eddy currents is valid. In the remainder of the paper, we set the frequency to 100 kHz and the particle radius to 80 µm, so that $a/\delta = 0.05$.

The next section presents and discusses the results of the simulations.

RESULTS AND DISCUSSION

DC conductivity

The computed effective conductivity at various volume fractions of particles is plotted on figure 3. Two regions can be clearly identified: for vanishing volume fractions, the effective conductivity is of the same order of magnitude as that of the matrix. A sudden change in

conductivity occurs past a volume fraction called the *percolation threshold*, around $\varphi_c = 0.27$. This value is in agreement with percolation theory of overlapping spheres [13]. The second region is then characterized by an effective conductivity of the same order of magnitude as the particle conductivity. In both regions, the scaling of the conductivity, σ_{eff}, is well described by the following shifted power laws [12]:

$$\sigma_{\text{eff}} = \sigma_{\text{mat}} \left(\frac{\varphi_c - \varphi}{\varphi_c}\right)^{t_m} \text{ for } \varphi < \varphi_c \,, \tag{8}$$

where σ_{mat} is the conductivity of the matrix, and:

$$\sigma_{\text{eff}} = \sigma_{\text{part}} \left(\frac{\varphi - \varphi_c}{1 - \varphi_c}\right)^{t_p} \text{ for } \varphi > \varphi_c \,, \tag{9}$$

where σ_{part} is the conductivity of the particles. The fitted values of the exponents are $t_m = -1.13 \pm 0.03$ and $t_p = 1.78 \pm 0.03$.

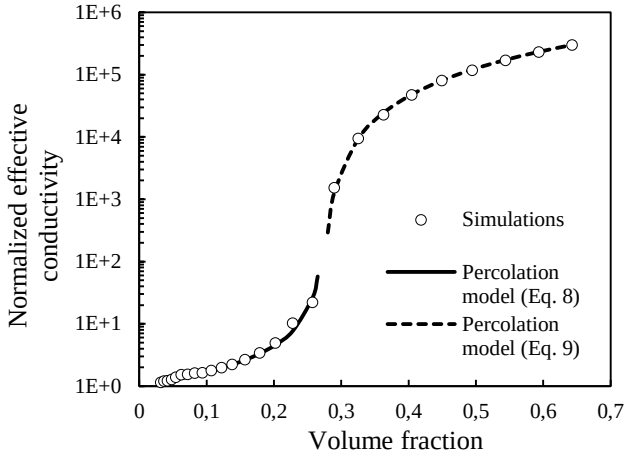

Figure 3. Effective conductivity as a function of volume fraction of particles.

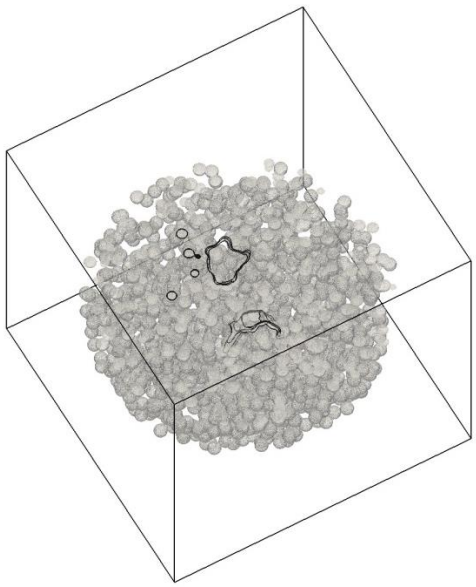

Figure 4. Current loops in a cluster of volume fraction 0.21.

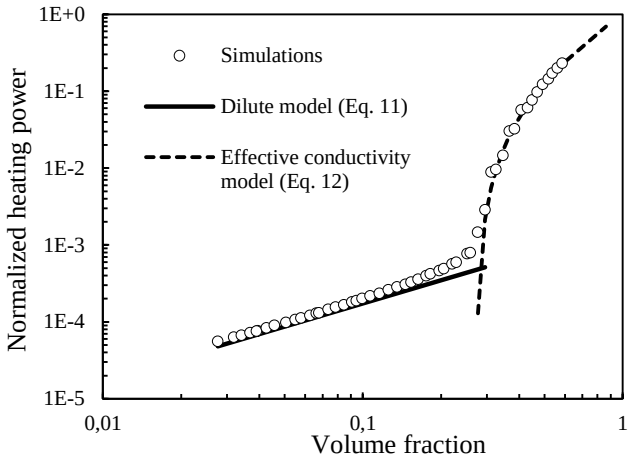

Figure 5. Normalized Joule power induced in the dispersion.

Induced power

Let us now turn our attention to the simulations of eddy currents. For these simulations, the particles are constrained in a spherical sub-region and an AC magnetic field is imposed at the boundary of the domain by enforcing an appropriate gradient of the vector potential. For illustration purposes, several current loops at a given volume fraction of 0.21 are plotted on figure 4. Some of the loops are confined in a single particle while some others span through an aggregate of several particles.

For each volume fraction, the time-averaged Joule loss is integrated over space. This heating power P is normalized by the value of the power that would be induced in a macroscopic metallic sphere of the same radius as the spherical sub-region. According to equation 1, the normalized power, P', is then given by:

$$P' = \frac{P}{\frac{2\pi\delta^3\omega B^2}{15\mu_0} f\left(\frac{r}{\delta}\right)}, \tag{10}$$

where r is the radius of the macroscopic sphere.

Results are reported in figure 5. For small volume fractions, the normalized Joule power is in good agreement with the analytical model of dilute dispersions (equation 3). Indeed, P' is proportional to the volume fraction of particles (solid curve):

$$P' = \frac{g\left(\frac{a}{\delta}\right)}{g\left(\frac{r}{\delta}\right)}\varphi. \tag{11}$$

In other words, at small volume fractions, the particles are heated independently of one another. As the volume fraction increases, wider current loops form, until the percolation threshold is reached in the cluster. Then the induced power is determined by the size of the cluster it-self, which is limited to the size of the simulation domain. However, it appears that the induced power in the spherical cluster is well described by the power induced in an equivalent homogeneous conducting sphere of the same radius. The normalized power can be written as:

$$P' = \frac{g\left(\frac{r}{\delta(\sigma_{\mathrm{eff}})}\right)}{g\left(\frac{r}{\delta}\right)}, \tag{12}$$

where $\delta(\sigma_{\text{eff}})$ is the skin depth in a medium of conductivity σ_{eff}. The corresponding effective conductivity is the volume-fraction-dependent DC effective conductivity above the percolation threshold given by equation 9. This model is plotted on figure 5 as a dashed curve.

In the intermediate region, that is, in the range $0.15 < \varphi < 0.3$, the Joule power is higher than both models. We can assume that this effect stems from small clusters that grow in size with the volume fraction, but whose surface enclosed by continuous conducting paths is still smaller than the simulation domain.

CONCLUSION

We studied the induction heating of a dispersion of conductive particles. We addressed the issue of the scaling of the heating power with respect to the volume fraction of the dispersed phase. 3D numerical simulations were performed on randomly distributed overlapping particles. For small volume fractions, the induced Joule power is in good agreement with an analytical model of dilute dispersions. As the volume fraction increases, wider current loops form, until the percolation threshold is reached. Then the induced power in the spherical aggregate is well described by the power induced in an equivalent sphere with a volume-fraction-dependent conductivity. Our approach can be used to simulate induction heating of more specific and realistic heterogeneous media, such as polydisperse, non-overlapping, dispersions, or three-phase materials.

ACKNOWLEDGEMENTS

This work was jointly funded by the CEA and AREVA.

REFERENCES

[1] Bayerl, T., Duhovic, M., Mitschang, P., Bhattacharyya, D. (2014) The heating of polymer composites by electromagnetic induction – A review. *Compos. Part A-Appl. S.* 57, 27–40.

[2] Mamunya, Y.P., Davydenko, V.V., Pissis, P., Lebedev, E.V. (2002) Electrical and thermal conductivity of polymers filled with metal powders. *European Polymer Journal*, 38, 1887–1897.

[3] Kim, H., Yarlagadda, S., Gillespie, J.W., Shevchenko, N.B., Fink, B.K. (2002) A study on the induction heating of carbon fiber reinforced thermoplastic composites. *Advanced Composite Materials*, 11, 71–80.

[4] Liu, Q., Yu, W., Schlangen, E., van Bochove, G. (2014) Unravelling porous asphalt concrete with induction heating. *Constr. Build. Mater.* 71, 152–157.

[5] Garcia, A., Schlangen, E., van de Ven, M., Liu, Q. (2009) Electrical conductivity of asphalt mortar containing conductive fibers and fillers. *Construction and Building Materials*, 23, 3175–3181.

[6] Menendez, J.A., Arenillas, A., Fidalgo, B., Fernandez, Y., Zubizarreta, L., Calvo, E.G., Bermudez, J.M. (2010) Microwave heating processes involving carbon materials. *Fuel Processing Technology*, 91, 1–8.

[7] Calabro, J.D., Huang, X., Lewis, B.G., Ramirez, A.G. (2010) Magnetically driven three-dimensional manipulation and inductive heating of magnetic-dispersion containing metal alloys. *Proceedings of the National Academy of Sciences*, 107, 4834–4839.

[8] Kim, D.H., Thai, Y.T., Nikles, D.E., Brazel, C.S. (2009) Heating of Aqueous Dispersions Containing Nanoparticles by Radio-Frequency Magnetic Field Induction. *IEEE Transactions on Magnetics*, 45, 64–70.

[9] Martinelli, J. R. & Sene, F. F. (2000) Electrical resistivity of ceramic–metal composite materials: application in crucibles for induction furnaces. *Ceram. Int.* 26, 325–335.

[10] Hussain, S., Barbariol, I., Roitti, S., Sbaizero, O. (2003) Electrical conductivity of an insulator matrix (alumina) and conductor particle (molybdenum) composites. *Journal of the European Ceramic Society*, 23, 315–321.
[11] Simonnet, C., Grandjean, A. (2005) Mixed ionic and electronic conductivity of RuO2–glass composites from molten state to glassy state. *Journal of Non-Crystalline Solids*, 351, 1611–1618.
[12] Clerc, J.P., Giraud, G., Laugier, J.M., Luck, J.M. (1990) The electrical conductivity of binary disordered systems, percolation clusters, fractals and related models. *Advances in Physics*, 39, 191–309.
[13] Torquato, S., Random Heterogeneous Materials, Springer, 2002.
[14] Bottauscio, O., Manzin, A., Piat, V.C., Codegone, M., Chiampi, M. (2006) Electromagnetic phenomena in heterogeneous media: Effective properties and local behaviour. *Journal of Applied Physics*, 100, 044902.
[15] Eberhard, J.P., (2005) Upscaling for the time-harmonic Maxwell equations with heterogeneous magnetic materials. *Phys. Rev. E*, 72, 036616.
[16] Vinogradov, A.P., Burokur, N., Zouhdi, S. (2009) Effective parameters of metal-dielectric composites: influence of eddy currents due to density fluctuations. *The European Physical Journal Applied Physics*, 46, 1–4.
[17] Bidinosti, C.P., Chapple, E.M., Hayden, M.E. (2007) The sphere in a uniform RF field—Revisited. *Concepts Magn. Reson.*, 31B, 191–202.
[18] Tomar, G., Gerlach, D., Biswas, G., Alleborn, N., Sharma, A., Durst, F., Welch, S.W.J., Delgado, A. (2007) Two-phase electrohydrodynamic simulations using a volume-of-fluid approach. *Journal of Computational Physics*, 227, 1267–1285.
[19] Rohlfs, W., Dietze, G.F., Haustein, H.D., Kneer, R. (2012) Two-phase electrohydrodynamic simulations using a volume-of-fluid approach: A comment. *Journal of Computational Physics*, 231, 4454–4463.
[20] Weller, H.G., Tabor, G., Jasak, H., Fureby, C. (1998) A tensorial approach to computational continuum mechanics using object-oriented techniques. *Comput. Phys.*, 12, 620–631.